

Synthesis of the 2Fe subcluster of the [FeFe]-hydrogenase H cluster on the HydF scaffold

Eric M. Shepard^a, Shawn E. McGlynn^a, Alexandra L. Bueling^a, Celestine S. Grady-Smith^b, Simon J. George^c, Mark A. Winslow^a, Stephen P. Cramer^b, John W. Peters^a, and Joan B. Broderick^{a,1}

^aDepartment of Chemistry and Biochemistry and the Astrobiology Biogeochemistry Research Center, Montana State University, Bozeman, MT 59717; ^bDepartment of Applied Science, University of California, Davis, CA 95616; and ^cPhysical Biosciences Division, Lawrence Berkeley National Laboratory, Berkeley, CA 94720

Edited* by JoAnne Stubbe, Massachusetts Institute of Technology, Cambridge, MA, and approved April 28, 2010 (received for review February 19, 2010)

The organometallic H cluster at the active site of [FeFe]-hydrogenase consists of a 2Fe subcluster coordinated by cyanide, carbon monoxide, and a nonprotein dithiolate bridged to a [4Fe-4S] cluster via a cysteinate ligand. Biosynthesis of this cluster requires three accessory proteins, two of which (HydE and HydG) are radical S-adenosylmethionine enzymes. The third, HydF, is a GTPase. We present here spectroscopic and kinetic studies of HydF that afford fundamental new insights into the mechanism of H-cluster assembly. Electron paramagnetic spectroscopy reveals that HydF binds both [4Fe-4S] and [2Fe-2S] clusters; however, when HydF is expressed in the presence of HydE and HydG (HydF^{EG}), only the [4Fe-4S] cluster is observed by EPR. Insight into the fate of the [2Fe-2S] cluster harbored by HydF is provided by FTIR, which shows the presence of carbon monoxide and cyanide ligands in HydF^{EG}. The thorough kinetic characterization of the GTPase activity of HydF shows that activity can be gated by monovalent cations and further suggests that GTPase activity is associated with synthesis of the 2Fe subcluster precursor on HydF, rather than with transfer of the assembled precursor to hydrogenase. Interestingly, we show that whereas the GTPase activity is independent of the presence of the FeS clusters on HydF, GTP perturbs the EPR spectra of the clusters, suggesting communication between the GTP- and cluster-binding sites. Together, the results indicate that the 2Fe subcluster of the H cluster is synthesized on HydF from a [2Fe-2S] cluster framework in a process requiring HydE, HydG, and GTP.

The reversible reduction of protons, a reaction central to bioenergy and fuel cell applications, is a conceptually simple but chemically challenging reaction. In biology, these reactions occur at unique organometallic metal centers that contain biochemically unusual nonprotein ligands such as carbon monoxide and cyanide. In the case of the [FeFe]-hydrogenase, the site of catalysis is a metal cluster, termed the H cluster, consisting of a [4Fe-4S] cubane bridged by a cysteine thiolate to a 2Fe unit coordinated by carbon monoxide, cyanide, and a bridging dithiolate ligand (Fig. 1) (1–6). The [FeFe]-hydrogenase is of particular interest for bioenergy applications because of its high catalytic rates of proton reduction; however, a limiting factor in its practical utilization is the lack of understanding of the biosynthesis of the organometallic active site cluster. Assembly of a catalytically competent H cluster requires the actions of three hydrogenase-specific accessory proteins, two of which (HydE and HydG) are radical S-adenosylmethionine (SAM) enzymes and the third of which (HydF) is a GTPase (7, 8). These accessory proteins are directed at synthesis of the 2Fe subcluster of the H cluster, which is subsequently transferred to the hydrogenase structural protein (HydA) containing a preformed [4Fe-4S] cluster (9, 10) to produce the active hydrogenase. The detailed stepwise mechanism of H-cluster assembly, as well as the specific roles of and interactions between the three accessory proteins in this assembly process, remains largely unknown. Herein we provide evidence that the 2Fe subcluster of the H cluster is synthesized on HydF from a [2Fe-2S] precursor by the activities of HydE and HydG and that GTP hydrolysis likely plays a role in the assembly of this precursor on HydF.

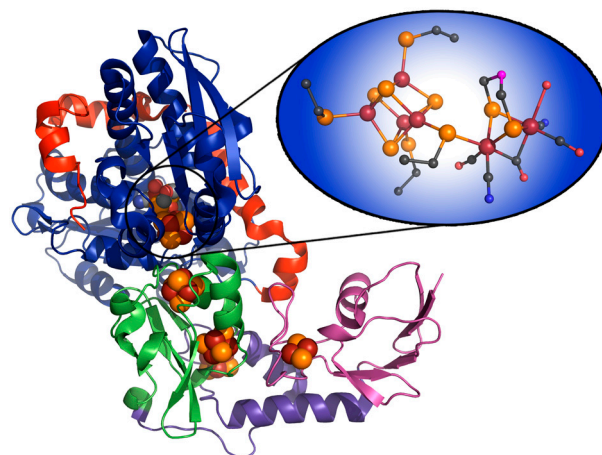


Fig. 1. Ribbon representation of *Clostridium pasteurianum* (Cpl) [FeFe] hydrogenase (Protein Data Bank ID code: 3C8Y) with the FeS clusters and H cluster shown as space filling models, and zoom of the H cluster as ball and stick representation. The Cpl domains are represented with different colors (C terminus: red, catalytic domain: blue, ferredoxin-like domains: green, purple, and magenta), and the FeS clusters and H cluster are colored to the following scheme: rust (Fe), orange (S), black (C), red (O), blue (N), and magenta (unknown).

Radical SAM enzymes are characterized by the presence of a site-differentiated iron-sulfur cluster that coordinates and reductively cleaves SAM to generate a 5'-deoxyadenosyl radical intermediate; the radical intermediate then abstracts a hydrogen atom from substrate to initiate a wide range of difficult chemical transformations whose details depend on the specific enzyme and substrate involved (11). Earlier biochemical studies of HydE and HydG from *Thermotoga maritima* demonstrated that both exhibited characteristic features of radical SAM enzymes, including the ability to bind iron-sulfur clusters and to catalyze the reductive cleavage of SAM (12). An X-ray crystal structure of HydE revealed the presence of a site-differentiated [4Fe-4S] cluster coordinated by SAM, as well as an additional [2Fe-2S] cluster (13). Given the sequence and biochemical data identifying HydE and HydG as radical SAM enzymes, our original hypothetical model for H-cluster assembly involved HydE- and HydG-catalyzed radical SAM chemistry on unknown substrates to synthesize

Author contributions: E.M.S., S.E.M., S.P.C., J.W.P., and J.B.B. designed research; E.M.S., S.E.M., A.L.B., C.S.G.-S., S.J.G., M.A.W., and S.P.C. performed research; E.M.S., S.J.G., S.P.C., J.W.P., and J.B.B. analyzed data; and E.M.S., J.W.P., and J.B.B. wrote the paper.

The authors declare no conflict of interest.

*This Direct Submission article had a prearranged editor.

¹To whom correspondence should be addressed at: Department of Chemistry and Biochemistry, Montana State University, 103 CBB, Bozeman, MT 59717. E-mail: jbroderick@chemistry.montana.edu.

This article contains supporting information online at www.pnas.org/lookup/suppl/doi:10.1073/pnas.1001937107/-DCSupplemental.

the CO, CN⁻, and bridging dithiolate ligands to the 2Fe subcluster of the H cluster; this 2Fe subcluster was proposed to be assembled on HydF and ultimately transferred to the hydrogenase structural protein (14). Consistent with this model, HydG has recently been shown to catalyze the degradation of tyrosine to produce cresol (15); this reaction is analogous to that of the radical SAM enzyme ThiH, which cleaves tyrosine to cresol and dehydroglycine in the thiamine biosynthetic pathway (16, 17). Rather than dehydroglycine, however, HydG produces cyanide as a second product of tyrosine cleavage (18). Although the substrate for HydE is unknown, we postulate that it is a common metabolite or amino acid; furthermore, the substrate must be present in *Escherichia coli* as well as the native organism, because heterologous expression of the accessory proteins in *E. coli* gives HydF that can activate HydA (14, 19). Phylogenetic analysis indicates a similarity to biotin synthase (BioB), suggesting that HydE may catalyze a BioB-like sulfur insertion to generate the bridging dithiolate ligand of the H cluster (18).

Studies of the [FeFe]-hydrogenase structural protein, HydA, have provided further insights into the roles of the accessory proteins in hydrogenase maturation. [FeFe]-hydrogenase heterologously expressed in the absence of accessory proteins (HydA^{ΔEFG}) can be activated in vitro by addition of *E. coli* cellular extracts in which HydE, HydF, and HydG are simultaneously coexpressed, and thus these three accessory proteins, together with substrates present in *E. coli*, are sufficient for assembly of the H cluster (19). Detailed spectroscopic and structural studies of HydA^{ΔEFG} have shown that it contains a [4Fe-4S] cluster and is poised to accept a 2Fe subcluster prior to activation by the accessory proteins (9, 10). We have also shown that HydF purified from *E. coli* in which all three accessory proteins were coexpressed (HydF^{EG}) was competent in HydA^{ΔEFG} activation, indicating that HydF acts as a scaffold or carrier protein during activation of HydA (20). The proposed scaffolding role for HydF was further supported by biochemical characterization of the enzyme from *T. maritima*, which demonstrated its ability to bind an iron-sulfur cluster and catalyze GTP hydrolysis (21). Together these findings suggest that the final step in hydrogenase maturation is the transfer of a 2Fe H cluster precursor from HydF to HydA, where it is bridged to the [4Fe-4S] cubane to generate the catalytically competent H cluster.

Whereas important advances have been made in understanding H-cluster assembly, key questions remain regarding this complex process. For example, the specific functions of and interactions between the three maturation proteins have not been clearly delineated. The nature of the 2Fe H-cluster precursor on HydF, and whether it is built directly on HydF by HydE and HydG or is instead assembled initially on one or both of the radical SAM enzymes prior to being transferred to HydF, is also not known. In addition, the role of GTP hydrolysis in H-cluster assembly is not understood. In order to clarify the role of HydF in hydrogenase maturation, we have used EPR and FTIR spectroscopic approaches to examine changes in cluster composition associated with the presence or absence of HydE and HydG during expression of HydF, and we have carried out a detailed study of GTP hydrolysis and its role in H-cluster assembly. Our results provide direct spectroscopic evidence for the expected CO and CN⁻ ligands of the 2Fe precursor bound to HydF and support a model in which the 2Fe subcluster of the H cluster is assembled directly on HydF via modification of a [2Fe-2S] cluster. Furthermore, we provide evidence that GTP hydrolysis plays a role in assembly of the 2Fe subcluster on HydF rather than in subcluster transfer from HydF to HydA.

Results

Spectroscopic Evidence for the Assembly of an H-cluster Precursor on HydF. HydF purified from *E. coli* contains iron-sulfur clusters, although the typical iron contents (approximately 1 per protein)

are indicative of substoichiometric loading given the evidence presented here for both [4Fe-4S] and [2Fe-2S] clusters in HydF (20). For the specific protein preparations used in the current study, the iron numbers were 0.98 (±0.18) Fe/protein for HydF^{ΔEG} and 0.85 (±0.1) Fe/protein for HydF^{EG}; both proteins as-isolated exhibited weak EPR signals characteristic of [3Fe-4S]⁺ clusters (Fig. S1). Despite these low iron numbers, we pursued spectroscopic studies directly on these purified proteins without utilizing in vitro cluster reconstitution, because our goal was to probe the cluster states of HydF relevant to the in vivo H-cluster assembly process. Reduced HydF^{ΔEG} exhibits a low-temperature EPR spectrum comprising a nearly axial signal characteristic of [4Fe-4S]⁺ clusters ($g_{\perp} = 1.89$ and $g_{\parallel} = 2.05$) overlapping a second signal ($g = 2.00, 1.96$) (Fig. 2). This second signal has different relaxation properties than the [4Fe-4S]⁺ signal (Fig. S24) and is most characteristic of a [2Fe-2S]⁺ cluster. In the presence of GTP, the intensity of both signals increases by a factor of 2 and the g value associated with the [2Fe-2S]⁺ component shifts from 2.00 to 2.01 (Fig. 2). The EPR spectral features of reduced HydF^{EG} (Fig. 2 and Fig. S2B, $g_{\perp} = 1.89$ and $g_{\parallel} = 2.05$) are similar to those described for HydF^{ΔEG}, with one key difference: The signal attributed to the [2Fe-2S]⁺ is essentially absent (>99% reduction in intensity). Similar to the observation for HydF^{ΔEG}, the EPR signal observed for reduced HydF^{EG} increases approximately 2-fold upon addition of GTP.

Three observations are of particular interest in these EPR studies. First, the EPR spectral features reported here are distinct from those reported previously for *Tm*HydF, which showed no effects upon GTP addition (21). Second, there is a loss of an EPR-active [2Fe-2S] cluster component when HydF is expressed in a background of HydE and HydG, which is consistent with HydE and HydG modifying a [2Fe-2S] cluster to an EPR-silent H-cluster precursor. Third, the presence of GTP significantly influences the EPR spectral properties, suggesting an interplay between the GTP- and cluster-binding sites on HydF.

FTIR spectroscopy has been utilized to further examine the changes in cluster content in HydF when it is expressed in a back-

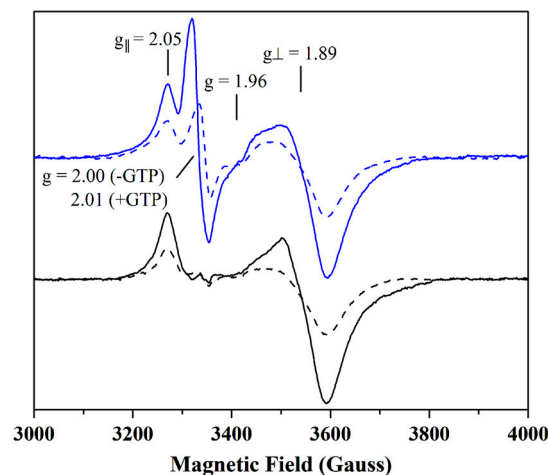


Fig. 2. Low-temperature (12 K) X-band EPR spectroscopic analysis of HydF^{ΔEG} and HydF^{EG}. The dashed blue line is photoreduced HydF^{ΔEG} in the presence of 5.3 mM MgCl₂ (500 μM protein in 500 mM KCl), and the solid blue line is the photoreduced enzyme in the presence of MgCl₂ (5 mM) and GTP (25 mM) (475 μM protein in 500 mM KCl). Reduced HydF^{ΔEG} spectra comprise a nearly axial signal characteristic of [4Fe-4S]⁺ clusters with $g_{\perp} = 1.89$ and $g_{\parallel} = 2.05$ overlapping a second signal with $g = 2.00$ and 1.96 (see text). The dashed black line is photoreduced HydF^{EG} in the presence of 5.3 mM MgCl₂ (220 μM protein in 440 mM NaCl and 40 mM KCl), and the solid black line is photoreduced HydF^{EG} in the presence of MgCl₂ (5 mM) and GTP (12.5 mM) (205 μM protein in 400 mM NaCl and 80 mM KCl). Reduced HydF^{EG} spectra comprise a nearly axial signal characteristic of [4Fe-4S]⁺ clusters with $g_{\perp} = 1.89$ and $g_{\parallel} = 2.05$.

ground of HydE and HydG and to address whether these changes are consistent with modification of the [2Fe-2S] cluster to a 2Fe subcluster coordinated by CO and CN⁻. FTIR is the technique of choice in this case because (i) it allows direct detection of the CO and CN⁻ diatomic ligands expected to be present on an H-cluster precursor and (ii) it is not dependent on the H-cluster precursor being in a paramagnetic oxidation state. The FTIR spectrum of HydF^{EG} (Fig. 3) shows sharp bands at 2,046, 2,027, 1,940, and 1,881 cm⁻¹, as compared to the bands at 2,106.5, 2,087, 2,007.5, 1,983, and 1,847.5 cm⁻¹ in holo-HydA (4). For the holo-[FeFe]-hydrogenase, the bands at 2,106.5 and 2,087 have been assigned to the cyanide ligands to the H cluster, whereas those at 2,007.5 and 1,983 cm⁻¹ have been assigned to terminal carbon monoxide ligands and the mode at 1,847.5 cm⁻¹ to a bridging CO ligand (4). Further, for the [FeFe]-hydrogenase and di-iron H-cluster model compounds, it has been shown that the CN⁻ ligand modes typically occur in the 2,110–2,025 cm⁻¹ range, whereas the CO ligand modes occur in the 2,015–1,850 cm⁻¹ (terminal CO) and 1,850–1,770 cm⁻¹ (bridging CO) regions of the spectrum (22–24). Given these assignments, we conclude that the 2,046 and 2,027 cm⁻¹ bands in HydF result from cyanide ligands, whereas those at 1,940 and 1,881 cm⁻¹ arise from terminal carbon monoxide ligands. Only two bands assigned to CO ligands are obvious in our FTIR spectrum of HydF^{EG}, although the weak residual intensity in the 1,800–1,830 cm⁻¹ region could be resulting from a bridging CO ligand. Alternatively, it is possible that the symmetry of the cluster precursor on HydF^{EG} gives rise to only two observed vibrational bands for three CO ligands on the cluster. The energies of the vibrational modes in HydF^{EG} are not identical to those in holo-HydA, which is not surprising given that the CO and CN⁻ vibrational modes are exquisitely sensitive not only to the electron richness of the metal (because of the fact that these ligands act as π -acids) but also to the polarity of the surrounding environment (25). Given the fact that these ligands are associated with a cluster precursor on HydF rather than the H cluster on HydA, one would expect some differences in the vibrational frequencies. In summary, our FTIR data provide clear evidence for the presence of CO and CN⁻ ligands, suggesting that the [2Fe-2S] cluster in HydF^{ΔEG} is converted to a CO- and CN⁻-ligated 2Fe subcluster. In contrast, the FTIR features characteristic of CO and CN⁻ ligation have not been observed in HydF^{ΔEG}. The combination of EPR and FTIR spectroscopy thus provide substantial evidence that the radical SAM enzymes HydE and HydG serve to modify a [2Fe-2S] cluster bound to HydF into

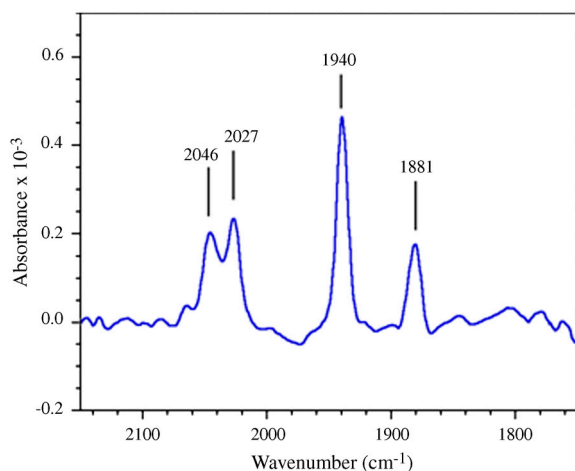


Fig. 3. FTIR spectrum of a HydF^{EG} sample (36 mg/mL) prepared under anaerobic conditions in a Coy chamber. The major observed bands are indicated. The bands at 1,940 and 1,881 cm⁻¹ are assigned to the $\nu(C=O)$ stretching vibrations of coordinated carbonyl groups whereas the bands at 2,046 and 2,027 cm⁻¹ are assigned to the $\nu(C=N)$ vibrations of bound cyanide (4).

the CO and CN⁻ ligated H-cluster precursor that is transferred to HydA to effect hydrogenase maturation.

GTPase Activity of HydF. HydF was originally shown by Posewitz and coworkers to contain a canonical nucleotide binding domain; this and subsequent mutagenesis studies suggested a role for GTP hydrolysis in H-cluster assembly (7, 8). Initial studies of HydF from *T. maritima* (*TmHydF*) surprisingly revealed very slow rates of GTP hydrolysis (21). In an effort to begin to delineate the role of GTP hydrolysis in H-cluster assembly, we undertook a detailed investigation of the GTPase activity of HydF from *Clostridium acetobutylicum* (*CaHydF*) expressed in *E. coli* either in the absence (HydF^{ΔEG}) or presence (HydF^{EG}) of the radical SAM accessory proteins and asked the question whether nucleotide hydrolysis plays a role in either synthesis of the H-cluster precursor on HydF or its transfer to HydA. Our results reveal that *CaHydF* is a specific GTPase (it is unable to hydrolyze ATP to ADP; see *SI Text*) with rates of GTP hydrolysis comparable to other characterized GTPases but much higher than previously characterized for *TmHydF* (Table 1).

The GTPase activity was found to be significantly affected by the nature of the monovalent cation in the reaction buffer (Table 1). The ability to gate GTPase activity through the use of different alkali metal salts appears to be directly linked to the ionic radius of the monovalent cation (Na⁺, 102 pm; K⁺, 138 pm; Rb⁺, 152 pm; Cs⁺, 167 pm), possibly indicating that a monovalent cation binding pocket exists near the active site. Activity in the presence of NH₄⁺, intermediate in size between K⁺ and Rb⁺, is slightly lower than that with K⁺, suggesting that direct coordination of ligands to the monovalent ion is an important determinant of activity. These results are comparable to those reported for MnmE, an *E. coli* GTPase involved in the modification of tRNAs, whose GTPase activity decreases in the following order: KCl, RbCl, CsCl, NaCl (26). X-ray structural characterization of MnmE revealed that K⁺ binds in close proximity to the GTP-binding pocket, forming a planar triangle with Mg²⁺ and Lys229 (located within the P-loop) around the β - γ bridging oxygens of GTP. The authors proposed that the K⁺ ion, which is not required for GTP binding, likely reduces the developing negative charge in the transition state and may play a role in helping to stabilize the position of the attacking water molecule; this is in fact analogous to the role of the “arginine finger” of the activating proteins required by some GTPases and thus may represent a mechanism by which some GTPases can act independently of an activating protein to achieve efficient GTP hydrolysis (26). In order to examine whether the kinetic salt effects observed with *CaHydF* were generally applicable to HydF from other sources, *TmHydF*^{EG} was expressed, purified, and assayed. Our preliminary analysis shows that the k_{cat} of 0.04 min⁻¹ (37 °C, NaCl-containing buffer) compares well to the reported value of 0.03 min⁻¹ for *TmHydF*^{ΔEG} (21), supporting the observation with *CaHydF* that the genetic background does not alter the GTPase activity of HydF (Table 1). Not surprisingly, the k_{cat} for *TmHydF*^{EG}

Table 1. Salt effects on HydF GTPase activity

Genetic background	Salt	Temp	k_{cat} (min ⁻¹)
HydF ^{EG}	KCl	30 °C	1.84 ± 0.10
HydF ^{ΔEG}	KCl	30 °C	1.76 ± 0.10
HydF ^{EG}	KCl	30 °C	1.77 ± 0.16*
HydF ^{ΔEG}	KCl	30 °C	2.08 ± 0.14*
HydF ^{EG}	NaCl	30 °C	0.09 ± 0.01
HydF ^{EG}	RbCl	30 °C	3.82 ± 0.29
HydF ^{EG}	CsCl	30 °C	0.19 ± 0.02
HydF ^{ΔEG}	NH ₄ Cl	30 °C	1.58 ± 0.10
HydF ^{ΔEG}	RbCl	30 °C	3.47 ± 0.25
HydF ^{ΔEG}	CsCl	30 °C	0.11 ± 0.01

*Assays run anaerobically in the MBraun box. All other assays were run under aerobic conditions.

increased as temperature was raised to 80 °C and showed salt effects (0.18 min⁻¹ NaCl; 0.44 min⁻¹ KCl) similar to those for *CaHydF*. Therefore it appears as though the nature of salt used in assay mixtures can act to gate the GTPase activity of HydF enzymes purified from various sources, although the magnitude of the effect may vary.

The role of the iron-sulfur cluster in GTP hydrolysis of *CaHydF* was examined by using metal-free and reconstituted HydF^{ΔEG}. HydF^{ΔEG} typically purifies with iron numbers of approximately 1 per protein (20). Treatment of HydF^{ΔEG} with EDTA results in a colorless protein containing no detectable iron using the spectrophotometric method of Fish (27). UV-visible analysis of the apo protein showed a protein-centered band at 280 nm and a weak band at 410 nm (Fig. S3) that would account for an Fe:protein ratio of ≈0.03, assuming an ϵ value of 15,000 M⁻¹ cm⁻¹ for a bound [4Fe-4S]²⁺ cluster. Reconstituted HydF^{ΔEG} samples are brown in color and showed strong ligand-to-metal charge transfer bands at 320 and 415 nm, a broad shoulder in the 600 nm region, and iron numbers up to 3.4 ± 0.5 (Fig. S3). The results in Table 2 clearly reveal that the cluster content of HydF has essentially no effect on the GTP hydrolysis kinetics.

GTP Hydrolysis and Cluster Transfer. In order to investigate the possibility that HydF-catalyzed GTP hydrolysis plays a role in transfer of an H-cluster precursor from HydF to HydA to generate active hydrogenase, hydrogenase activation assays were carried out that utilized both a nonhydrolyzable GTP analog and the salt effects on GTPase kinetics described above to modulate GTPase activity, and the effects on hydrogenase activation were examined. Activation assays containing HydA^{ΔEFG}, HydF^{EG}, and either GDP, GTP, or the nonhydrolyzable GTP analog guanosine-5'-[β,γ -imido] triphosphate were performed to examine the effect of GTP hydrolysis on HydA^{ΔEFG} activation. As shown in Fig. 4, no significant changes in the amount of active hydrogenase were observed despite the different experimental conditions that tested "GTPase-on" (KCl) and "GTPase-off" (NaCl) states in the presence or absence of product, substrate, or a nonhydrolyzable substrate analog. The small differences observed at later time points are thought to arise from slight variations during experimental setup, because this assay is extremely sensitive to minor variables and errors become magnified as the H₂ production assay proceeds; it is not uncommon to obtain 5% variation in

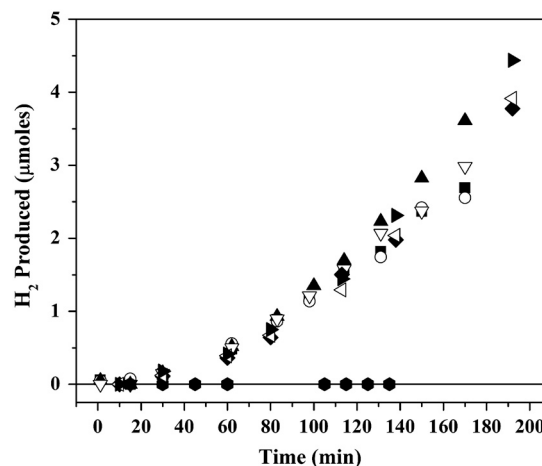


Fig. 4. H₂ evolution assays to probe the effects of guanosine nucleotides on the activation of HydA^{ΔEFG} by HydF^{EG}. All reactions contained 1.1 mM MgCl₂ and 500 mM of an alkali metal salt; the identity of the alkali metal salt and the guanosine nucleotide varied as follows: NaCl and no guanosine nucleotide (solid square); NaCl and 110 μM [β,γ -imido]-GTP (circle); KCl and no guanosine nucleotide (solid triangle and solid diamond); KCl and 110 μM [β,γ -imido]-GTP (down triangle); KCl and 110 μM GTP (left triangle); KCl and 110 μM GDP (solid right triangle); control containing HydF^{EG} without HydA^{ΔEFG} (KCl) (solid hexagon).

levels among vials with identical reaction conditions at the same time points. Regardless, it is clear that there are no substantial effects of these various conditions on the activation of HydA^{ΔEFG}, indicating that the GTPase functionality of HydF^{EG} is unrelated to its ability to activate immature HydA^{ΔEFG}.

Further support for this conclusion is provided in the observation that the presence of HydA^{ΔEFG} has no effect on the rate of GTP hydrolysis by HydF (Table 2). This result is in contrast to the effects of HydE and HydG on the GTPase activity of HydF; both of these accessory proteins are found to increase HydF GTPase activity by approximately 50%. Together, the lack of effect of GTP on HydA^{ΔEFG} activation by HydF^{EG}, the lack of effect of HydA on the GTPase activity of HydF, and the observed effect of HydE and HydG on the GTPase activity of HydF all point to a role for GTP hydrolysis not in 2Fe subcluster transfer to HydA but rather in the earlier chemical steps in which HydE and HydG interact with HydF to synthesize the H-cluster precursor.

Discussion

The presence of NTPase enzymes in the assembly of metal clusters appears to be an emerging theme in metallobiochemistry, although definitive roles have not yet been established in many cases (28–34). HydF contains an N-terminal GTPase domain comprised of the Walker A P-loop and Walker B Mg²⁺ binding motifs (8), as well as a C-terminal domain containing the conserved amino acids CXH_{X44-53}HCXXC comprising the putative ligands for an iron-sulfur cluster (7). GTP binding and/or hydrolysis is essential to HydF's role in HydA maturation, because mutations in the Walker P-loop prevent the formation of active HydA in vitro (8). Although the precise role of GTP binding/hydrolysis in H-cluster assembly remains uncertain, the results described herein provide important insights. First, whereas the presence of the iron-sulfur clusters is not required for GTP hydrolysis by HydF, GTP significantly affects the EPR spectral properties of the iron-sulfur clusters, suggestive of a direct communication between the iron-sulfur cluster and GTP-binding domains. Second, although the presence of HydA has no effect on the rate of HydF-catalyzed GTP hydrolysis, both HydE and HydG increase the rate of GTP hydrolysis by 50%. This result suggests that GTP binding and/or hydrolysis are associated with interactions of HydF with the other accessory proteins rather than with the hydrogenase structural protein. Such

Table 2. The effect of metal cluster content and presence of hydrogenase gene products on HydF GTPase activity

Protein	Salt	Temp	k_{cat} (min ⁻¹)
HydF ^{ΔEG}	KCl	30 °C	2.43 ± 0.36
HydF ^{ΔEG} Stripped	KCl	30 °C	2.33 ± 0.28
HydF ^{ΔEG} Reconstituted	KCl	30 °C	2.30 ± 0.31
HydF ^{EG}	KCl	30 °C	1.98 ± 0.17*
HydF ^{EG} + HydE ^{EG}	KCl	30 °C	3.03 ± 0.18 [†] , [‡]
HydF ^{EG} + HydG ^{EG}	KCl	30 °C	3.12 ± 0.11 [†]
HydF ^{EG} + HydA ^{ΔEFG}	KCl	30 °C	2.21 ± 0.28 [†]
HydF ^{EG} + HydA ^{ΔEFG}	KCl/NaCl	30 °C	1.34 ± 0.09 [†] , [§]
HydF ^{ΔEG} + HydA ^{ΔEFG}	KCl/NaCl	30 °C	1.53 ± 0.09 [†] , [§]

*The experiments run with HydE, HydG, and HydA in this table were performed with a stock of HydF from a different preparation than what was used to measure the salt effects in Table 1.

[†]HydE, HydF, and HydG are from *C. acetobutylicum* and HydA is from *C. pasteurianum* (Cpl). Enzyme incubations were performed anaerobically with 1 μM HydF^{EG} and 10 μM hydrogenase gene product, respectively.

[‡]The k_{cat} value reported for the HydF^{EG} experiment is the result of a single set of experimental data. We attempted to repeat the experiment three additional times but in each case HydF^{EG} precipitated. All other data reported in this table are the result of either two or three independent experiments.

[§]The salt ratio for the HydF^{EG} experiment is 122 mM NaCl to 378 mM KCl, whereas the salt ratio for the HydF^{ΔEG} experiment is 176 mM NaCl to 324 mM KCl.

interactions were previously inferred from the copurification of HydE and HydG with HydF (20). Most importantly, our *in vitro* activation studies in the presence and absence of GTP, GDP, and [β - γ -imido] GTP under both GTPase-on and GTPase-off salt conditions demonstrate that GTP hydrolysis is not required for the activation of HydA ^{Δ EF Δ G} by HydF^{EG}. We therefore suggest that GTP binding and hydrolysis is associated with the interprotein interactions involved in cluster assembly on HydF, perhaps by inducing structural changes in the enzyme that result in altered interactions with the other accessory proteins, and/or by perturbation of the cluster environment where the H-cluster precursor is assembled. This latter possibility is directly analogous to the case for the monovalent cation-activated GTPase MnmE (26), which has a separate active site for tRNA modification that is perturbed by GTP binding and hydrolysis. The nitrogenase Fe protein provides another comparable example wherein MgATP binding induces alterations in the microenvironment around the [4Fe-4S] cluster 15 Å away (35–37).

The nature of the 2Fe H-cluster precursor assembled by the Hyd accessory proteins is illuminated by the current work. Comparative EPR studies reveal that the cluster composition of HydF is changed when the protein is produced concomitantly with HydE and HydG, with a [2Fe-2S] on HydF cluster becoming EPR-silent when the three accessory proteins are expressed together. FTIR spectroscopic analysis reveals that HydF^{EG} contains CO and CN⁻ ligands with spectroscopic properties similar to those of holo-HydA. These observations are consistent with a model in which HydE and HydG catalyze radical SAM chemistry that ultimately results in the modification of a [2Fe-2S] cluster on HydF, such that it resembles the 2Fe subcluster of the H cluster (Fig. 5) and has spectroscopic features that are distinct from a canonical [2Fe-2S] cluster. While this work was in progress, the group of Happe and Lubitz reported FTIR and EPR spectroscopic characterization of *C. acetobutylicum* (*Ca*) HydF overexpressed in *C. acetobutylicum* in the presence of *Ca*HydE and *Ca*HydG (38). Their *Ca*HydF^{EG} shows similar EPR *g* values, assigned to a [4Fe-4S]⁺ cluster, as well as similar vibrational modes assigned to a CO- and CN⁻-ligated 2Fe cluster.

HydE and HydG are required for the transformation of the [2Fe-2S] cluster on HydF to an H-cluster precursor; however, insight into the precise catalytic functions of these radical SAM enzymes is just beginning to emerge. We have recently demonstrated that HydG can synthesize CN⁻ via the radical decomposition of tyrosine (18), and this ligand together with CO is presumably delivered to HydF to produce the H-cluster precursor that is ultimately transferred to HydA. The synthesis of carbon monoxide and cyanide by HydG would then suggest that the function of HydE is to synthesize the remaining nonprotein ligand of the H cluster, the bridging dithiolate. Given the results presented herein, we propose that HydE catalyzes insertion of the bridging sulfides from the [2Fe-2S] cluster on HydF into C-H bonds of a substrate in a manner analogous to the accepted mechanism for biotin synthase (39, 40). This modification of the [2Fe-2S] cluster would dramatically alter the cluster properties, allowing for

addition of the CO and CN⁻ ligands by HydG to generate the final H-cluster precursor. The results presented herein provide evidence that HydF is not simply a carrier of the 2Fe subcluster to the H cluster but is a true assembly scaffold upon which the 2Fe subcluster is built from a [2Fe-2S] cluster precursor by the activities of HydE and HydG.

Experimental Procedures

Protein Expression and Purification. Constructs encoding Hyd maturation proteins from *C. acetobutylicum* were transformed into *E. coli*-BL21 (DE3) (Stratagene) cells for protein expression, as described in ref. 20 with slight modifications. Cell lysis and protein purification were carried out under anaerobic conditions in a Coy chamber, as described in ref. 20 with slight modifications. Detailed procedures for both expression and purification are provided in *SI Text*.

GTPase Kinetic Assays. As-isolated HydF^{EG} and HydF ^{Δ EG} were assayed for their ability to hydrolyze GTP under a variety of experimental conditions, including variations in temperature, the nature of salt present in the assay mixture, the presence and absence of O₂, and the effects of HydA ^{Δ EF Δ G}, HydG^{EF}, and HydE^{FG}, respectively. Assay conditions were as follows: alkali metal salt (400 mM final), GTP (2 mM final); guanosine 5' triphosphate sodium salt, Sigma, minimum 95% HPLC), MgCl₂ (2 mM final), DTT (2 mM final), HydF^{EG} and HydF ^{Δ EG} (7–14 μ M final). Additionally, to determine the effects of accessory and structural hydrogenase proteins on the GTPase activity of HydF, assays were set up in the presence of 10 μ M HydA ^{Δ EF Δ G}, HydG^{EF}, and HydE^{FG}, respectively, with 1 μ M HydF^{EG}. Last, as-isolated HydF ^{Δ EG} was compared to metal-free and reconstituted forms of HydF ^{Δ EG} in order to examine the effects of metal cluster content on GTPase activity. Assays were run either in an anaerobic chamber (Mbraun, <1 ppm O₂) or on the benchtop, and temperature was controlled by using an IsoTemp block (Fisher). Further details of assay conditions are provided in *SI Text*.

HPLC Analysis. At given time points, aliquots of GTPase assay mixtures were removed, quenched by addition of 1 M HCl, and analyzed by reverse-phase HPLC. GDP and GTP peak areas were integrated and compared to control assays run in parallel. Details on the sample prep, chromatography, and calculations are described in *SI Text*.

Determination of the Effects of GTPase Activity on [FeFe]-Hydrogenase Activation. To determine whether GTPase activity was associated with the maturation of HydA ^{Δ EF Δ G} by HydF^{EG}, enzyme samples were assayed in KCl- and NaCl-containing buffers (50 mM Hepes, pH 7.4, 500 mM salt), in the presence or absence of GDP, GTP, or the nonhydrolyzable GTP-analog guanosine-5'-[β , γ -imido] triphosphate (trisodium salt, Sigma, 91% HPLC). As described in ref. 20, assays are performed by combining purified inactive HydA ^{Δ EF Δ G} with purified HydF^{EG} in the presence of methyl viologen and dithionite. Details are provided in *SI Text*.

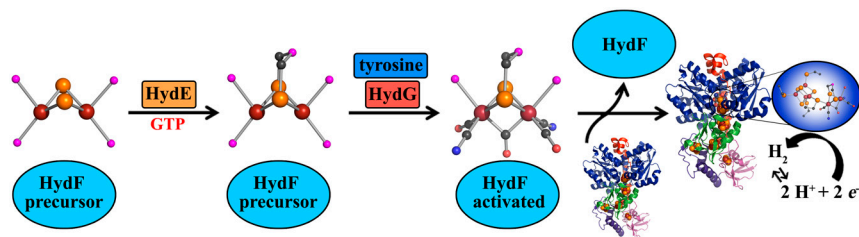


Fig. 5. Proposed biosynthetic pathway for the H-cluster of [FeFe] hydrogenases. HydE utilizes an unknown substrate to synthesize the bridging dithiolate ligand on a [2Fe-2S] core on HydF in a step possibly utilizing GTP hydrolysis. This cluster intermediate is further processed by HydG, which utilizes tyrosine to synthesize CO and CN⁻ ligands, thus completing synthesis of the 2Fe unit of the H-cluster on the HydF scaffold. The activated form of HydF then interacts with HydA ^{Δ EF Δ G} and transfers the 2Fe cluster, thereby affording the holo [FeFe]-hydrogenase.

EPR Sample Preparation and Spectroscopic Analysis. EPR samples were prepared in an MBraun box at O₂ levels <1 ppm by using the methods described in *SI Text*. Low-temperature EPR spectra were collected by using a Bruker EMX X-band spectrometer equipped with a liquid helium cryostat and temperature controller from Oxford instruments. Typical EPR parameters were: sample temperature, 12 K; microwave frequency, 9.37 GHz; microwave power, 1.85 mW; time constant, 81.92 msec; sweep time, 167.77 sec.

FTIR Sample Preparation and Spectroscopic Analysis. FTIR samples were prepared under anaerobic conditions in a Coy anaerobic chamber containing approximately 3% H₂ atmosphere. FTIR spectra were measured by using a Bruker IFS/66S FTIR spectrometer interfaced to a home-built stopped-flow drive system with the sample cuvette and drive system maintained inside an anaerobic chamber (Belle Technology, O₂ < 1.1 ppm) as described elsewhere (41). The IR cuvette was thermostatted at

25 °C. For these measurements, protein sample in 50 mM Hepes pH 7.4 buffer containing 500 mM NaCl were introduced on only one side of the drive system, with the other side loaded with buffer. Spectra were measured at 4 cm⁻¹ resolution. The IR cuvette path length was calibrated at 47.6 μm. Arbitrary background corrections were applied to yield flat baselines for measured spectra.

ACKNOWLEDGMENTS. The authors thank Dr. Robin Gerlach for running ICP-MS samples and Dr. Anatoli Naumov for supplying the *Thermotoga* HydF constructs. We thank William Broderick for insightful discussions. The authors thank the National Aeronautics and Space Administration Astrobiology Institute for support of the Montana State University Astrobiology Biogeochemistry Research Center (NNA08CN85A to J.W.P. and J.B.B.). S.E.M. is supported by an National Science Foundation Integrative Graduate Education and Research Traineeship Fellowship (Montana State University Program in Geobiological Systems, DGE 0654336). The authors acknowledge funding for the establishment of the Environmental and Biofilm Mass Spectrometry Facility through the Defense University Research Instrumentation Program (DURIP, Contract W911NF0510255).

- Peters JW, Lanzilotta WN, Lemon BJ, Seefeldt LC (1998) X-ray crystal structure of the Fe-only hydrogenase (CpI) from *Clostridium pasteurianum* to 1.8 Å resolution. *Science* 282:1853–1858.
- Nicolet Y, Piras C, Legrand P, Hatchikian CE, Fontecilla-Camps JC (1999) *Desulfovibrio desulfuricans* iron hydrogenase: The structure shows unusual coordination to an active site Fe binuclear center. *Structure* 7:13–23.
- Nicolet Y, et al. (2001) Crystallographic and FTIR spectroscopic evidence of changes in Fe coordination upon reduction of the active site of the Fe-only hydrogenase from *Desulfovibrio desulfuricans*. *J Am Chem Soc* 123:1596–1601.
- Pierik AJ, Hulstein M, Hagen WR, Albracht SPJ (1998) A low-spin iron with CN and CO as intrinsic ligands forms the core of the active site in [Fe]-hydrogenases. *Eur J Biochem* 258:572–578.
- Silakov A, Wenk B, Reijerse E, Lubitz W (2009) ¹⁴N HYSCORE investigation of the H-cluster of [FeFe]-hydrogenase: evidence for a nitrogen in the dithiol bridge. *Phys Chem Chem Phys* 11:6592–6599.
- Pandey AS, Harris TV, Giles LJ, Peters JW, Szilagyi RK (2008) Dithiomethylether as a ligand in the hydrogenase H-cluster. *J Am Chem Soc* 130:4533–4540.
- Posewitz MC, et al. (2004) Discovery of two novel radical S-adenosylmethionine proteins required for the assembly of an active [Fe] hydrogenase. *J Biol Chem* 279:25711–25720.
- King PW, Posewitz MC, Ghirardi ML, Seibert M (2006) Functional studies of [FeFe] hydrogenase maturation in an *Escherichia coli* biosynthetic system. *J Bacteriol* 188:2163–2172.
- Mulder DW, et al. (2009) Activation of HydA^{ΔEFG} requires a preformed [4Fe-4S] cluster. *Biochemistry* 48:6240–6248.
- Mulder DM, et al. (2010) Stepwise [FeFe]-hydrogenase H-cluster assembly revealed in the structure of HydA^{ΔEFG}. *Nature* doi:10.1038/nature08993.
- Frey P, Hegeman A, Ruzicka F (2008) The radical SAM superfamily. *Crit Rev Biochem Mol Biol* 43:63–88.
- Rubach JK, Brazzolotto X, Gaillard J, Fontecave M (2005) Biochemical characterization of the HydE and HydG iron-only hydrogenase maturation enzymes from *Thermotoga maritima*. *FEBS Lett* 579:5055–5060.
- Nicolet Y, et al. (2008) X-ray structure of the [FeFe]-hydrogenase maturase HydE from *Thermotoga maritima*. *J Biol Chem* 283:18861–18872.
- Peters JW, Szilagyi RK, Naumov A, Douglas T (2006) A radical solution for the biosynthesis of the H-cluster of hydrogenase. *FEBS Lett* 580:363–367.
- Pilet E, et al. (2009) The role of the maturase HydG in [FeFe]-hydrogenase active site synthesis and assembly. *FEBS Lett* 583:506–511.
- Kriek M, Martins F, Challand MR, Croft A, Roach PL (2007) Thiamine biosynthesis in *Escherichia coli*: Identification of the intermediate and by-product derived from tyrosine. *Angew Chem Int Ed Engl* 46:9223–9226.
- Kriek M, et al. (2007) Thiazole synthase from *Escherichia coli*: An investigation of the substrates and purified proteins required for activity *in vitro*. *J Biol Chem* 282:17413–17423.
- Driesener RC, et al. (2010) [FeFe]-Hydrogenase cyanide ligands derived from S-adenosylmethionine dependent cleavage of tyrosine. *Angew Chem* 49:1687–1690.
- McGlynn SE, et al. (2007) *In vitro* activation of [FeFe] hydrogenase: new insights into hydrogenase maturation. *J Biol Inorg Chem* 12:443–447.
- McGlynn SE, et al. (2008) HydF as a scaffold protein in [FeFe] hydrogenase H-cluster biosynthesis. *FEBS Lett* 582:2183–2187.
- Brazzolotto X, et al. (2006) The [Fe-Fe]-hydrogenase maturation protein HydF from *Thermotoga maritima* is a GTPase with an iron-sulfur cluster. *J Biol Chem* 281:769–774.
- Razavet M, Davies SC, Hughes DL, Pickett CJ (2001) {2Fe3S} clusters related to the di-iron sub-site of the H-centre of all-iron hydrogenases. *Chem Commun* 847–848.
- Roseboom W, De Lacey AL, Fernandez VM, Hatchikian EC, Albracht SPJ (2006) The active site of the [FeFe]-hydrogenase from *Desulfovibrio desulfuricans*. II. Redox properties, light sensitivity and CO-ligand exchange as observed by infrared spectroscopy. *J Biol Inorg Chem* 11:102–118.
- Silakov A, Kamp C, Reijerse E, Happe T, Lubitz W (2009) Spectroelectrochemical characterization of the active site of the [FeFe]-hydrogenase HydA1 from *Chlamydomonas reinhardtii*. *Biochemistry* 48:7780–7786.
- Nakamoto K (1997) *Infrared and Raman Spectra of Inorganic Coordination Compounds. Applications in Coordination, Organometallic, and Bioinorganic Chemistry* (Wiley, New York).
- Scrima A, Wittinghofer A (2006) Dimerisation-dependent GTPase reaction of MnmE: How potassium acts as GTPase-activating element. *EMBO J* 25:2940–2951.
- Fish WW (1988) Rapid colorimetric micromethod for the quantitation of complexed iron in biological samples. *Method Enzymol* 158:357–364.
- Chandramouli K, Johnson MK (2006) HscA and HscB stimulate [2Fe-2S] cluster transfer from IscU to apoferritin in an ATP-dependent reaction. *Biochemistry* 45:11087–11095.
- Vickery LE, Cupp-Vickery JR (2007) Molecular chaperones HscA/Ssq1 and HscB/Jac1 and their roles in iron-sulfur protein maturation. *Crit Rev Biochem Mol Biol* 42:95–111.
- Boyd JM, Pierik AJ, Netz DJA, Lill R, Downs DM (2008) Bacterial ApbC can bind and effectively transfer iron-sulfur clusters. *Biochemistry* 47:8195–8202.
- Boyd JM, Sondelki JL, Downs DM (2009) Bacterial ApbC protein has two biochemical activities that are required for *in vivo* function. *J Biol Chem* 284:110–118.
- Amutha B, et al. (2008) GTP is required for iron-sulfur cluster biogenesis in mitochondria. *J Biol Chem* 283:1362–1371.
- Leach MR, Zhang JW, Zamble DB (2007) The role of complex formation between the *Escherichia coli* hydrogenase accessory factors HypB and SlyD. *J Biol Chem* 282:16177–16186.
- Zambelli B, et al. (2005) UreG, a chaperone in the urease assembly process, is an intrinsically unstructured GTPase that specifically binds Zn²⁺. *J Biol Chem* 280:4684–4695.
- Ryle MJ, Lanzilotta WN, Seefeldt LC (1996) Elucidating the mechanism of nucleotide-dependent changes in the redox potential of the [4Fe-4S] cluster in nitrogenase iron protein: The role of phenylalanine 135. *Biochemistry* 35:9424–9434.
- Jang SB, Jeong MS, Seefeldt LC, Peters JW (2004) Structural and biochemical implications of single amino acid substitutions in the nucleotide-dependent switch regions of the nitrogenase Fe protein from *Azotobacter vinelandii*. *J Biol Inorg Chem* 9:1028–1033.
- Chiu H-J, et al. (2001) MgATP-bound and nucleotide-free structures of a nitrogenase protein complex between the Leu 127(Δ)-Fe-protein and the MoFe-protein. *Biochemistry* 40:641–650.
- Czech I, Silakov A, Lubitz W, Happe T (2010) The [FeFe]-hydrogenase maturase HydF from *Clostridium acetobutylicum* contains a CO and CN- ligated iron cofactor. *FEBS Lett* 584:638–642.
- Ugulava NB, Sacanell CJ, Jarrett JT (2001) Spectroscopic changes during a single turnover of biotin synthase: Destruction of a [2Fe-2S] cluster accompanies sulfur insertion. *Biochemistry* 40:8352–8358.
- Berkovitch F, Nicolet Y, Wan JT, Jarrett JT, Drennan CL (2004) Crystal structure of biotin synthase, an S-adenosylmethionine-dependent radical enzyme. *Science* 303:76–79.
- Thorneley RNF, George SJ (2000) *Prokaryotic Nitrogen Fixation: A Model System for Analysis of a Biological Process*, ed EW Triplett (Horizon Scientific, Wymondham, UK).